PCP
PLANT & CELL PHYSIOLOGY

Special Issue – Regular Paper

Identification of *kaonashi* Mutants Showing Abnormal Pollen Exine Structure in *Arabidopsis thaliana*

Toshiya Suzuki, Kanari Masaoka, Masatomo Nishi, Kenzo Nakamura and Sumie Ishiguro*

Department of Biological Mechanisms and Functions, Graduate School of Bioagricultural Sciences, Nagoya University, Nagoya 464-8601, Japan

Exine, the outermost architecture of pollen walls, protects male gametes from the environment by virtue of its chemical and physical stability. Although much effort has been devoted to revealing the mechanism of exine construction, still little is known about it. To identify the genes involved in exine formation, we screened for Arabidopsis mutants with pollen grains exhibiting abnormal exine structure using scanning electron microscopy. We isolated 12 mutants, *kaonashi1* (*kns1*) to *kns12*, and classified them into four types. The type 1 mutants showed a collapsed exine structure resembling a mutant of the callose synthase gene, suggesting that the type 1 genes are involved in callose wall synthesis. The type 2 mutant showed remarkably thin exine structure, presumably due to defective primexine thickening. The type 3 mutants showed defective tectum formation, and thus type 3 genes are required for primordial tectum formation or biosynthesis and deposition of sporopollenin. The type 4 mutants showed densely distributed baculae, suggesting type 4 genes determine the position of probacula formation. All identified *kns* mutants were recessive, suggesting that these *KNS* genes are expressed in sporophytic cells. Unlike previously known exine-defective mutants, most of the *kns* mutants showed normal fertility. Map-based cloning revealed that *KNS2*, one of the type 4 genes, encodes sucrose phosphate synthase. This enzyme might be required for synthesis of primexine or callose wall, which are both important for probacula positioning. Analysis of *kns* mutants will provide new knowledge to help understand the mechanism of biosynthesis of exine components and the construction of exine architecture.

Keywords: *Arabidopsis thaliana* • Exine • *kaonashi* • Pollen grain • Sucrose phosphate synthase.

Abbreviations: dCAPS, derived cleaved amplified polymorphic sequence; EMS, ethyl methanesulfonate RT–PCR, reverse transcription–PCR; SEM, scanning electron microscopy; SNP, single nucleotide polymorphism; SPS, sucrose phosphate synthase; SSLP, simple sequence length polymorphism; TEM, transmission electron microscopy.

Introduction

The surface structure of pollen grains (pollen walls) shows extreme diversity among higher plant species. In Arabidopsis (*Arabidopsis thaliana*), pollen grains have one of the most typical surface structures, namely a reticulate sculpture with uniform mesh size (**Fig. 1A**). This structure consists of inner intine, mainly made of cellulose and pectin, and outer exine, composed of sporopollenin, presumed to be a polymer of fatty acid derivatives and phenylpropanoids (**Fig. 1B**) (McCormick 1993, Scott 1994, Owen and Makaroff 1995, Paxson-Sowders et al. 1997, Scott et al. 2004, Morant et al. 2007). Exine is composed of inner nexine and outer sexine. Sexine has a three-dimensional structure composed of many columns called baculae and a roof-like tectum that gives a reticulate appearance to the pollen surface. Nexine is divided into outer nexine I and inner nexine II based on differences in chemical components. Nexine I is composed of sporopollenin, like sexine, whereas the components of nexine II are unknown. In addition, a pollen coat, composed of adhesive compounds containing proteins and lipids, accumulates in cavities of the exine.

Exine architecture is probably important to protect male gametes in the pollen grains from physical shock, chemical penetration and bacterial infection during pollination. Furthermore, in Arabidopsis, the lipophilic components of exine are required for pollen–stigma adhesion (Zinkl et al. 1999).

*Corresponding author: E-mail, guronyan@agr.nagoya-u.ac.jp; Fax, +81-52-789-4094.

Plant Cell Physiol. 49(10): 1465–1477 (2008) doi:10.1093/pcp/pcn131, available online at www.pcp.oxfordjournals.org

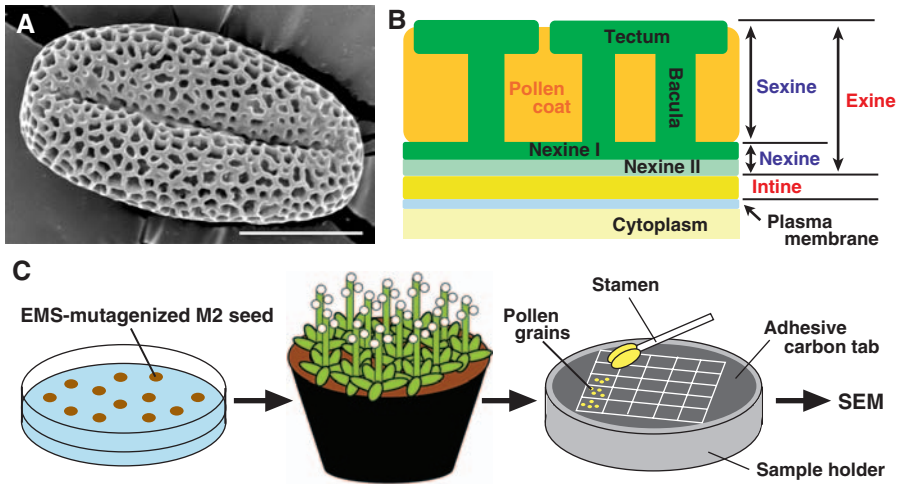

Fig. 1 Surface structure of mature pollen grains of wild-type Arabidopsis and the strategy used for mutant screening. (A) Wild-type pollen grains observed by SEM. The reticulate sculpture of exine can be observed. Bar = 10 μm. (B) Diagram of the pollen surface structure composed of inner intine, outer exine, and pollen coat filling the cavities of the exine sculpture. Exine is divided into sexine (outermost tectum and column-like baculae) and nexine (nexine I and innermost nexine II). (C) Procedure for mutant screening. M_2 seeds were sown on an agar plate and grown for 2 weeks, and then seedlings were transplanted to vermiculite and grown to maturity. When flowers opened, a stamen was detached from a fully opened flower of each plant and pollen grains were put on an SEM sample holder. After coating with Pt and Pd, the surface structure of the pollen grains was observed by SEM.

The formation of pollen surface structure has been investigated for >40 years using transmission electron microscopy (TEM). A model of pollen wall development based on observation of *Lilium* has been proposed (Scott 1994). A similar process has been observed in Arabidopsis (Owen and Makaroff 1995, Paxson-Sowders et al. 1997), which is summarized as follows. Immediately after meiosis, four microspores derived from each pollen mother cell form a tetrad, in which the microspores are surrounded with a callose (β-1,3-glucan) wall. Then primexine, mainly composed of cellulose, is formed between the plasma membrane of each microspore and the callose wall. Next, a part of the primexine is converted to a probacula, a column-like structure that is receptive to sporopollenin predicted to be secreted by microspores. Deposition of sporopollenin elongates the probacula and forms the tectum. With the dissolution of the callose wall, developing baculae and tectum are exposed to the locular fluid and now accept tapetum-derived sporopollenin. To complete pollen wall formation, nexine I, nexine II and intine are subsequently formed and the primexine matrix disappears.

An increasing number of genes participating in exine formation have been reported in Arabidopsis. The *CALLOSE SYNTHASE5* (*CALS5*)/*LESS ADHERENT POLLEN1* (*LAP1*) gene encodes a callose synthase that is indispensable for callose wall formation at the tetrad stage. The exine structure of *cals5*/*lap1* pollen grains is severely deformed, suggesting that the callose wall is essential for the formation of the exine structure (Dong et al. 2005, Nishikawa et al. 2005). Both the *NO EXINE FORMATION1* (*NEF1*) gene encoding a putative plastid integral membrane protein and the *RUPTURED POLLEN GRAIN1* (*RPG1*) gene encoding a plasma membrane protein are required for primexine formation (Ariizumi et al. 2004, Guan et al. 2008). The *DEFECTIVE IN EXINE FORMATION 1* (*DEX1*) and *TRANSIENT DEFECTIVE EXINE 1* (*TDE1*)/*DE-ETIOLATED 2* (*DET2*) genes are required for formation of the probacula. The DEX1 protein is a novel membrane protein that is required for anchoring sporopollenin to the surface of microspores (Paxson-Sowders et al. 1997, Paxson-Sowders et al. 2001). The *TDE1*/*DET2* gene is involved in brassinosteroid biosynthesis, indicating that brassinosteroids control the initial process of exine formation (Ariizumi et al. 2008). Three genes are involved in sporopollenin biosynthesis. The *MALE STERILITY2* (*MS2*) gene is predicted to encode fatty acyl reductase (Aarts et al. 1997). The *FACELESS POLLEN-1* (*FLP1*)/*WAX2*/*YORE-YORE* (*YRE*)/*ECERIFERUM3* (*CER3*) gene encodes a putative lipid transfer protein and is also required for the formation of pollen coat and epicuticular wax on stems and fruits (Ariizumi et al. 2003, Rowland et al. 2007). The *CYP703A2* gene encodes a protein having lauric acid hydroxylase activity (Morant et al. 2007). Morant et al. (2007) proposed a model of sporopollenin structure in which medium-chain saturated fatty acids and phenylpropanoids are polymerized through ester and ether linkages. Transcription factors required for exine formation have also been identified. The AtMYB103/MS188 protein is a MYB transcription factor that directly regulates the expression of both the *MS2* gene and the callase-related gene *A6* (Zhang et al. 2007). It has been

suggested that the MALE STERILITY1 (MS1)/HACKLY MICROSPORE (HKM) protein, containing a PHD-finger motif, is required for transcriptional regulation of genes involved in primexine formation, sporopollenin biosynthesis and other tapetal functions (Ariizumi et al. 2005, Ito et al. 2007, Yang et al. 2007).

Although an increasing number of genes involved in exine formation have been identified as noted above, the molecular mechanisms concerning the construction of the complex exine architecture are not yet fully understood. In particular, the biosynthetic pathways of primexine and sporopollenin, the molecular components of the probacula, the mechanisms of secretion and deposition of sporopollenin, the determination of the pattern of probacula distribution and the construction of the reticulate structure of the tectum are largely unknown. Furthermore, many of the mutants described above show severe defects not only in exine formation but also in overall structure and viability of developing microspores. Therefore, it cannot be ruled out that the defects in exine formation in these mutants are not direct effects of gene disruption but rather result from the reduced viability of microspores. In this study, we screened mutagenized Arabidopsis using scanning electron microscopy (SEM) to identify novel mutants that had pollen grains with abnormal exine structure. We identified 12 such mutants and found that the pollen viability of most of them was not affected. We describe phenotypic classification of these mutants, the proposed normal function of the mutated genes and molecular identification of one of the genes.

Results

TEM observation of exine development in wild-type Arabidopsis

To study the mechanism of exine development in Arabidopsis, we first observed the process of exine formation in wild-type Landsberg *erecta* (Ler) plants by TEM. We harvested a series of flower buds from inflorescences, and prepared sections of them to observe every stage of pollen development from pollen mother cells to mature pollen grains. **Fig. 2** presents the process of pollen development and exine formation at the same magnification throughout the process.

At the stage of pollen mother cells, a thick matrix was observed between the primary cell wall and plasma membrane (**Fig. 2A, B**). This matrix was identified as callose in a previous report (Owen and Makaroff 1995). However, the matrix was difficult to stain with a callose-specific stain, aniline blue (data not shown), indicating that it is different from a typical callose wall. This matrix contained many electron-dense fibrils, whereas the callose wall in tetrads looked uniform and did not contain such fibrils (**Fig. 2B, D**). No exine or primexine structure was observed at this stage.

At the tetrad stage immediately after meiosis, each microspore in the tetrads was separated by a callose wall 0.5 µm thick. A layer of primexine surrounding each microspore had formed between the plasma membrane and callose wall. Deposition of sporopollenin to form probaculae began at the distal part of the primexine adjacent to the callose wall and became a columnar structure on protrusions of undulating plasma membrane (**Fig. 2C, D**). No particular structure was observed on the indented surface of the undulating plasma membrane, at which an electron-opaque material termed a 'spacer' was identified in *Brassica campestris* (Fitzgerald et al. 1995). Tapetum-derived sporopollenin was deposited on the outer surface of each tetrad (**Fig. 2C**).

At the early unicellular stage when free microspores were released into the locules, an electron-dense thin layer of nexine I appeared just outside the plasma membrane (**Fig. 2E, F**). Developing baculae stood on the nexine I. The height of the bacula in this stage was less than half that of mature pollen grains. Exine began to grow tangentially along the outer surface of the primexine to form the tectum. Numerous fibrous materials were observed in the locules (**Fig. 2E, F**), which are assumed to supply the sporopollenin from tapetal cells to developing exine (Owen and Makaroff 1995, Paxon-Sowders et al. 1997).

At the late unicellular stage when many vacuoles are formed in the microspores, the whole exine architecture had enlarged to its maximum size, and development of the exine structure except for nexine II was almost completed (**Fig. 2G, H**). The thickness of exine, equivalent to the length of the bacula, was somewhat greater than that of mature exine, although the circumference of microspores at this stage was nearly half that of mature pollen grains (**Fig. 2G, I**). Primexine had already disappeared (**Fig. 2G, H**). A similar structure was observed in an electron micrograph of the microspore at the bicellular stage, when a generative cell appeared (**Fig. 4A, B**). The number of probaculae or baculae along the circumference of pollen grains is constant during pollen development, suggesting that the number of baculae is determined at the initial stage of probacula formation.

By the stage when tricellular mature pollen grains had grown to 20 µm in diameter, electron-translucent nexine II had formed underneath the nexine I to complete exine development (**Fig. 2I, J**). As a consequence of the increased surface area of pollen grains, the distance between baculae had increased. A layer of intine appeared between nexine II and the plasma membrane, and pollen coats were deposited on the exine cavities (**Fig. 2I, J**).

Comparison of the electron micrographs at the same magnification clearly indicated that both thickness and height of the bacula and tectum increased along with the development of pollen grains until the late unicellular stage.

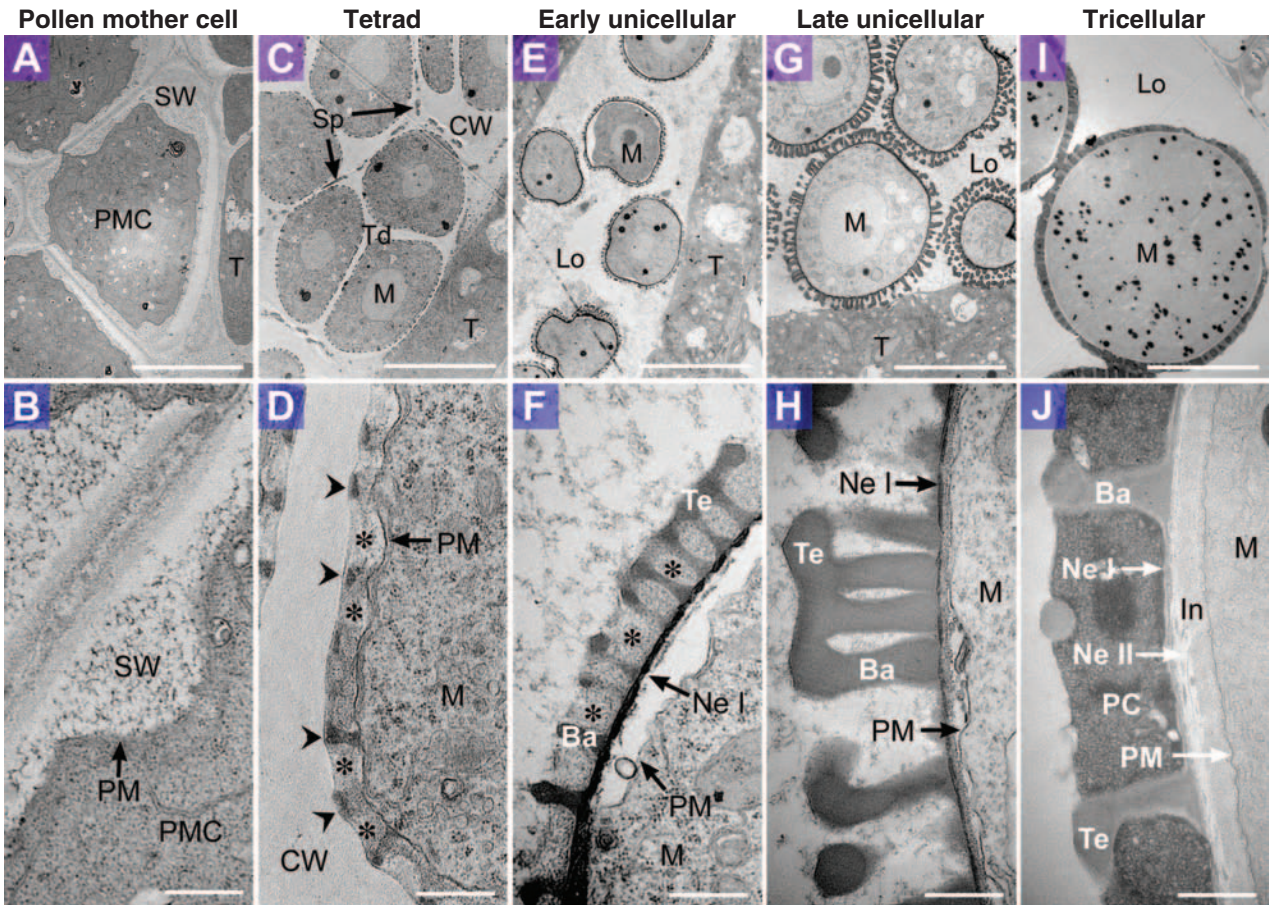

Fig. 2 Exine development in wild-type Arabidopsis. Transmission electron micrographs showing sections of developing pollen grains in wild-type Arabidopsis (Ler). Micrographs in the top row have the same magnification (A, C, E, G, I) (bars = 10 µm), and those in the bottom row have the same magnification (B, D, F, H, J) (bars = 0.5 µm). (A, B) Pollen mother cells. Each pollen mother cell is surrounded by secondary cell wall. (C, D) Tetrads. Primexine (asterisks) appears between the plasma membrane and callose wall, and the probaculae (arrowheads) are visible above the raised positions of the undulating plasma membrane. Sporopollenin is deposited more densely at the distal part of the probaculae, adjacent to the callose wall. (E, F) Microspores in the early unicellular stage. Feeble tectum, baculae and nexine I are visible. Primexine remains in the cavity of developing exine (asterisks). (G, H) Microspores in the late unicellular stage. Sexine formation is almost complete. (I, J) Tricellular mature pollen grains. Nexine II and intine have formed. Ba, bacula; CW, callose wall; In, intine; Lo, locule; M, microspore; Ne I, nexine I; Ne II, nexine II; PC, pollen coat; PM, plasma membrane; PMC, pollen mother cell; SP, sporopollenin deposited on the outer surface of tetrads; SW, secondary cell wall; T, tapetal cell; Td, tetrad; Te, tectum.

Isolation of *kaonashi* mutants showing abnormal exine structure

In order to identify Arabidopsis mutants defective in exine formation, we screened approximately 2,000 ethyl methanesulfonate (EMS)-mutagenized M_2 individuals by observation of their pollen surface structure with SEM (**Fig. 1C**). To make the screening easier, we used the Ler accession as the background strain, because this strain has short inflorescence stems growing upright without shoring. Twelve mutants with various abnormalities in exine structure were identified and named *kaonashi* (*kns*), which means 'faceless' in Japanese.

The phenotypic and genetic characteristics of all identified *kns* mutants, *kns1*–*kns12*, are summarized in **Table 1**. Based on characteristics of exine architecture, we classified these mutants into four types, described below. The mutants showed no visible phenotype other than the pollen abnormality.

kns1 and *kns11* are type 1 mutants with collapsed exine structure

Mature pollen grains of both *kns1* and *kns11* mutants, referred to as type 1, displayed collapsed exine structures, in which the tectum had disappeared and the bacula was deformed into a globular protrusion (**Fig. 3A, B**). The normal reticulate structure of exine partially remained on the surface of *kns1* pollen grains, whereas the defect of *kns11* exine was more remarkable and no normal bacula or tectum was identified. By TEM of developing microspores at the

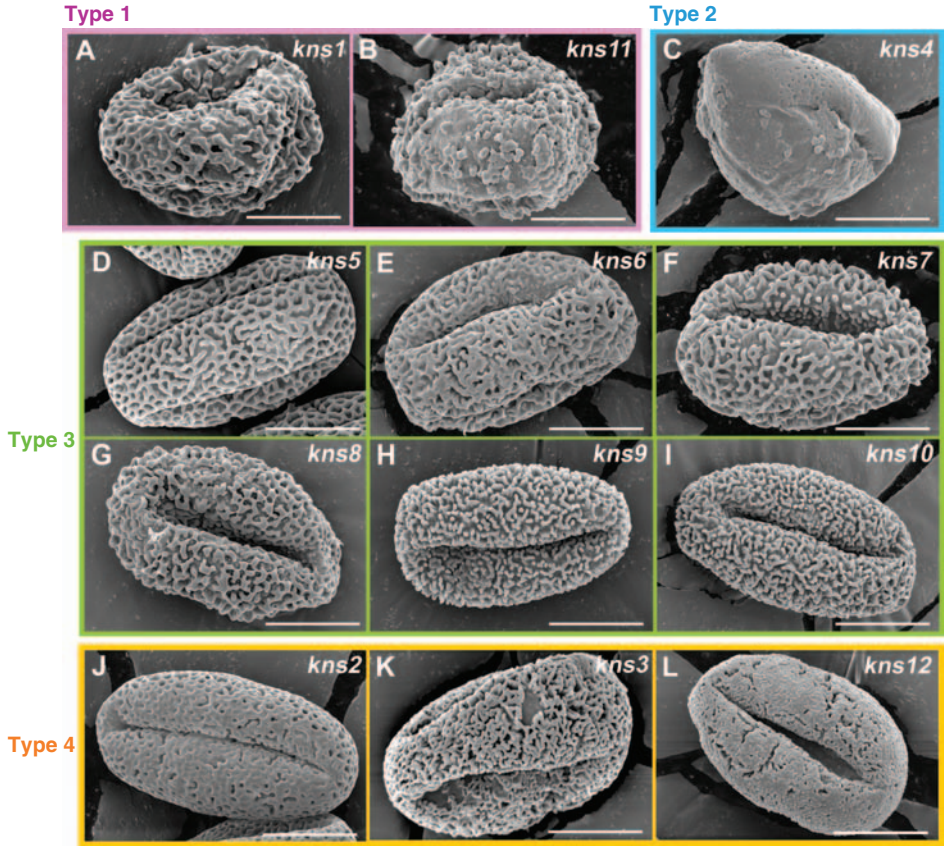

Fig. 3 Phenotypes of *kaonashi* mutants and their classification. Scanning electron micrographs of pollen grains isolated from each mutant. (A, B) The type 1 mutants, *kns1* and *kns11*, show highly collapsed exine structure. (C) The type 2 mutant, *kns4*, has remarkably thin exine. (D–I) The type 3 mutants, *kns5*, *kns6*, *kns7*, *kns8*, *kns9* and *kns10*, show defects in tectum formation. (J–L) The type 4 mutants, *kns2*, *kns3* and *kns12*, show abnormal distribution of bacula location. Bars = 10 μm.

bicellular stage, we confirmed that *kns1* exine lacked tectum but contained sparse but thick bacula-like structures (**Fig. 4C, D,** asterisks). The nexine I in *kns1* was indistinguishable from that of the wild type, while many unidentified globular structures appeared on the surface of nexine (**Fig. 4D,** arrowheads). A significant number of *kns1* microspores had begun to collapse and their contents had leaked out into the locules (**Fig. 4C**). Mature pollen grains of both *kns1* and *kns11* were reduced in number and size, and were distorted. In particular, pollen grains of the *kns11* mutant were severely withered and sterile. However, *kns1* pollen grains are fertile, meaning the mutant produced self-pollinated seed in an amount comparable with the wild type (**Fig. 5B; Table 1**).

kns4 is a type 2 mutant with a thin exine layer

We defined thin exine mutants as type 2. Under observation by SEM, the surface of *kns4* pollen grains was smooth and seemingly lacked the exine structure, although the reticulate pattern was faintly observable on the surface (**Fig. 3C**). Surprisingly, however, TEM revealed that *kns4* had an extremely thin exine layer, which was less than half as thick (0.5 μm) as wild-type exine (**Fig. 4E, F**). All three elements comprising the exine structure (nexine, bacula and tectum) were identified in the *kns4* exine, although the baculae were much shorter than that of the wild type, and the thickness of nexine I was not uniform in *kns4* pollen grains. Many mature pollen grains of *kns4* withered and aggregated even when observed under a dissecting microscope in wet conditions (data not shown). Nevertheless, the *kns4* mutant produced an amount of self-pollinated seed comparable with the wild type, suggesting that the fertility of *kns4* pollen grains is normal (**Table 1**). As a reticulate pattern was observed on the *kns4* pollen surface, it seemed likely that exine patterning was completed normally. The *KNS4* gene may be involved in the thickening of primexine, the thickness of which determines the height of exine.

kns5, kns6, kns7, kns8, kns9 and *kns10* are type 3 mutants showing defective tectum formation

The mutants showing defects in tectum formation were referred to as type 3, which included six mutants, *kns5*, *kns6*,

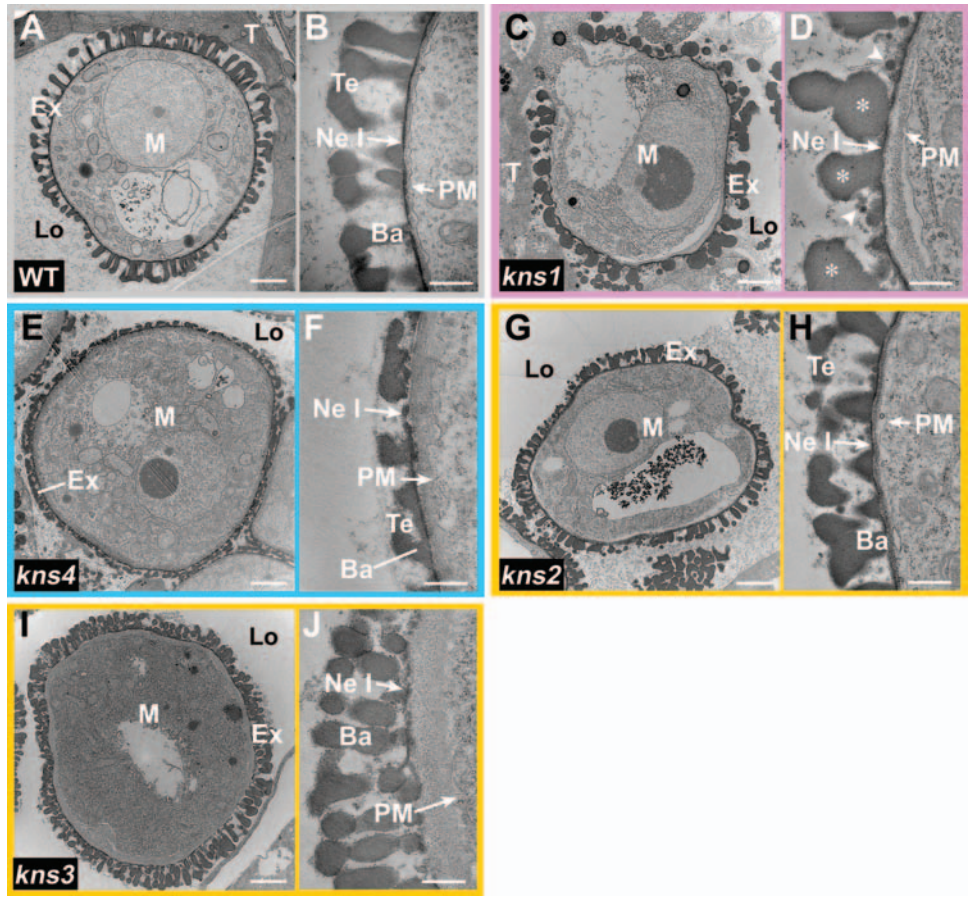

Fig. 4 Exine structure in *kns* microspores. Transmission electron micrographs indicating cross-sections of wild-type and *kns* microspores at the bicellular stage. (A, B) Wild type (Ler). Exine construction has been completed except for nexine II. (C, D) *kns1*. Deformed baculae (asterisks) can be observed, but tectum is missing. Many globular structures (arrowheads) appear on the surface of nexine I. (E, F) *kns4*. The exine structure of *kns4* is less than half the thickness of wild-type exine. (G, H) *kns2*. (I, J) *kns3*. Microspores of these mutants are surrounded by densely distributed baculae. Bars = 2 µm (A, C, E, G, I) and 0.5 µm (B, D, F, H, J). Ba, bacula; Ex, exine; Lo, locule; M, microspore; Ne I, nexine I; PM, plasma membrane; T, tapetal cell; Te, tectum.

Table 1 Phenotypic and genetic characteristics of identified *kaonashi* mutants

			Segregation in F_2[b,c]			
Mutation	**Phenotype**	**Pollen fertility[a]**	**Normal**	**Aberrant**	**Both**	**Map position[c]**
kns1	Type 1	++	486	84	0	Chr 2
kns2	Type 4	++	424	70	0	Chr 5
kns3	Type 4	++	287	48	0	Chr 5
kns4	Type 2	++	275	86	0	Chr 1
kns5	Type 3	++	nd	nd	nd	nd
kns6	Type 3	++	112	31	0	Chr 1
kns7	Type 3	++	280	86	0	Chr 1
kns8	Type 3	++	nd	nd	nd	nd
kns9	Type 3	++	152	19	0	Chr 3
kns10	Type 3	++	101	20	0	Chr 3
kns11	Type 1	–	nd	nd	nd	nd
kns12	Type 4	++	95	34	0	Chr 5

[a] ++, fully fertile; –, sterile.
[b] Normal, aberrant, and both categories represent the number of F_2 plants that produced only normal pollen grains, only aberrant pollen grains, and both normal and aberrant pollen grains, respectively.
[c] nd, not determined.

kns7, *kns8*, *kns9* and *kns10* (**Fig. 3D–I**). The tectum was partially broken on *kns5* pollen grains, which had the mildest phenotype in this class (**Fig. 3D**). The tectum of *kns6*, *kns7* and *kns8* pollen grains was broken into many pieces and some baculae were exposed. The *kns7* tectum was simply broken, whereas swollen baculae and very fine tectum-like threads were observed on *kns8* pollen surfaces (**Fig. 3F, G**). *kns6* showed an intermediate phenotype between that of *kns7* and *kns8* (**Fig. 3E**). The exine structure of *kns9* and *kns10* pollen grains was very similar, and they showed the most remarkable phenotypes in this class. The tectum had almost disappeared and the baculae were clearly exposed (**Fig. 3H, I**). The overall size, shape and fertility of pollen grains of all six mutants were comparable with those of wild-type pollen grains (**Table 1**).

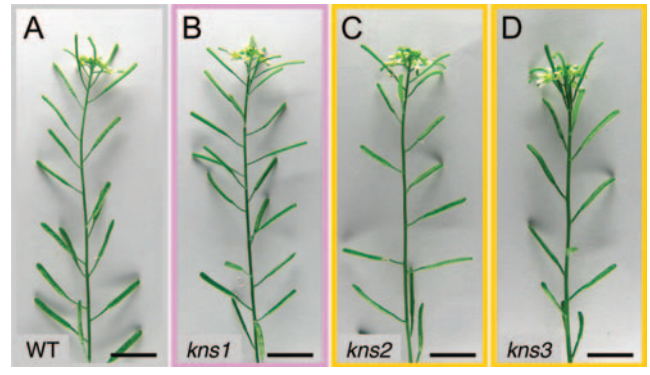

Fig. 5 Fertility of *kns* mutants. Primary inflorescences of 40-d-old plants. (A) Wild type (Ler). (B) *kns1*. (C) *kns2*. (D) *kns3*. Bars = 1 cm.

kns2, *kns3* and *kns12* are type 4 mutants showing abnormal bacula distribution

The mutants displaying abnormal mesh size in the exine structure were designated type 4, including *kns2*, *kns3* and *kns12* (**Fig. 3J–L**). *kns2* pollen grains were covered with reticulate exine structures, the mesh size of which was slightly smaller than that of the wild type (**Fig. 3J**). The number of baculae in the circumference of cross-sections of *kns2* pollen grains appearing on electron micrographs was 76 ± 4 ($n = 8$), which was slightly but significantly higher than that of the wild type (70 ± 5, $n = 9$) (**Fig. 4G, H**). In addition, pollen grains with a fragmented tectum were occasionally identified from *kns2* plants, resembling the type 3 phenotype (**Supplementary Fig. S1**). The surface of *kns3* pollen grains showed a similar but much finer mesh pattern (**Fig. 3K**). The number of baculae in the pollen circumference was 102 ± 7 ($n = 4$), indicating that the density of baculae had increased to 1.5 times that of the wild type (**Fig. 4I, J**). Tectum was barely discernable and nexine I looked discontinuous. A thick layer between nexine I and the plasma membrane, where nexine II and intine will form at a later stage, was also remarkable in *kns3* pollen grains (**Fig. 4J**). In addition, small patches were occasionally observed in which nexine I was exposed (**Fig. 3K**). The exine of *kns12* pollen grains consisted of dense baculae and a small fragmented tectum (**Fig. 3L**). Some pollen grains of *kns3* and *kns12* were entirely distorted, in contrast to the almost normal *kns2* pollen grains. Nevertheless, pollen grains of all these three mutants were fully fertile (**Fig. 5C, D**; **Table 1**).

Segregation of *kns* mutations

We manually pollinated the pistils of all *kns* mutants with wild-type Columbia (Col-0) pollen to generate F_1 plants. All F_1 plants produced only pollen grains that were normal in exine structure (data not shown). In the F_2 generation, 3:1 segregation between wild-type plants (that produced only normal pollen grains) and mutant plants (that produced only aberrant pollen grains) was observed for *kns4*, *kns6*, *kns7* and *kns12* (**Table 1**). For *kns1*, *kns2*, *kns3*, *kns9* and *kns10*, the ratio was 5:1 to 8:1, due to difficulty in distinguishing between normal and aberrant pollen grains (*kns2*), linkage with a dwarf mutation (*kns9*) or undetermined reasons (*kns1*, *kns3* and *kns10*). We never observed F_2 plants that produced both normal and aberrant pollen grains simultaneously (**Table 1**). Therefore, we concluded that the *kns* mutations are recessive, and that the corresponding wild-type *KNS* genes are expressed in diploid cells in anthers, such as pollen mother cells and tapetal cells. Similar segregation analysis of other *kns* mutants is in progress. We used the Col-0 wild type, instead of Ler (the background strain of the mutants), for crosses because such F_2 plants could be used directly for rough mapping of the mutations.

Rough mapping of *kns* mutations

To characterize newly isolated mutants with overlapping phenotypes, it is important to determine their allelic relationships. However, it is not easy to carry out test crossing in a round-robin fashion. Therefore, instead of cross-based allelism tests, we carried out chromosome mapping of each mutation. We crossed all *kns* mutants with wild-type Col-0 plants and obtained F_2 seeds. Around 40 F_2 plants displaying each mutant phenotype were collected and used for PCR-based rough mapping. The results are shown in **Table 1**.

Identification of the *KNS2* gene by map-based cloning

kns2 is a type 4 mutant, and its pollen grains show a high density of bacula formation. To shed light on the mechanism of exine pattern formation, we attempted to identify the *KNS2* gene. By rough mapping with 32 F_2 plants showing the *kns2* phenotype, we found that the *KNS2* locus is located on chromosome 5, between the markers CIW14 and CA72. We then identified 45 F_2 plants having recombination sites

between CIW14 and CA72, and used them for fine mapping. Finally, we mapped *KNS2* to a 49 kb region on chromosome 5, and identified a unique mutation in the At5g11110 gene by sequencing of this 49 kb region (**Fig. 6A**). The *kns2* (hereafter referred to as *kns2-1*) mutation caused a C to T substitution in the coding region of this gene, which resulted in substitution of Pro596 for leucine in the corresponding protein (**Fig. 6A**). We obtained a T-DNA insertion line (SALK_088752) of this gene (designated *kns2-2*), in which the T-DNA insertion was located within the coding region of the first exon, between nucleotide positions 140 and 143 (numbered from A of the initiation codon) (**Fig. 6A**). Plants homozygous for the *kns2-2* mutation showed the same phenotype as that of the original *kns2-1* mutant (**Fig. 6B**). Thus, we concluded that the *KNS2* gene is At5g11110. This gene, previously reported as *AtSPS2F* and *AtSPS5.2* (Langenkamper et al. 2002, Lutfiyya et al. 2007), encodes the enzyme sucrose phosphate synthase (SPS), catalyzing the rate-limiting step of sucrose biosynthesis from UDP-glucose and fructose-6-phosphate. Pro596 is located in the glycosyltransferase I domain of this protein and is highly conserved among the SPS enzymes of plants and cyanobacteria (Lutfiyya et al. 2007). Therefore, the *kns2-1* mutation seems likely to disrupt the function of this gene. Reverse transcription–PCR (RT–PCR) revealed that the *KNS2* gene is highly expressed in flowers and flower buds [consisting of stage 12 and younger according to the definition of Smyth et al. (1990)] as well as in roots, but not in leaves (**Fig. 6C**). Furthermore, *KNS2* expression was detected in stage 10/11 anthers, which included unicellular and bicellular microspores, and increased in older anthers, suggesting that its expression is required for microspore development throughout all stages (**Fig. 6C**).

Discussion

At the beginning of this study, we observed the process of exine formation in wild-type Arabidopsis by TEM to establish a basis for investigating exine development. Our observations are consistent with previous reports (Scott 1994, Owen and Makaroff 1995, Paxson-Sowders et al. 1997, Paxon-Sowders et al. 2001), although our series of electron micrographs clearly indicated that the exine enlarges dramatically during the early phase of microspore development. We found that the deposition of sporopollenin onto the probaculae began at the distal part of the primexine, adjacent to the callose wall at protrusions of the undulating microspore plasma membrane, suggesting that the sporopollenin is supplied predominantly from tapetal cells rather than microspores. It should be noted that the sporopollenin deposition at the membrane protrusions might be an

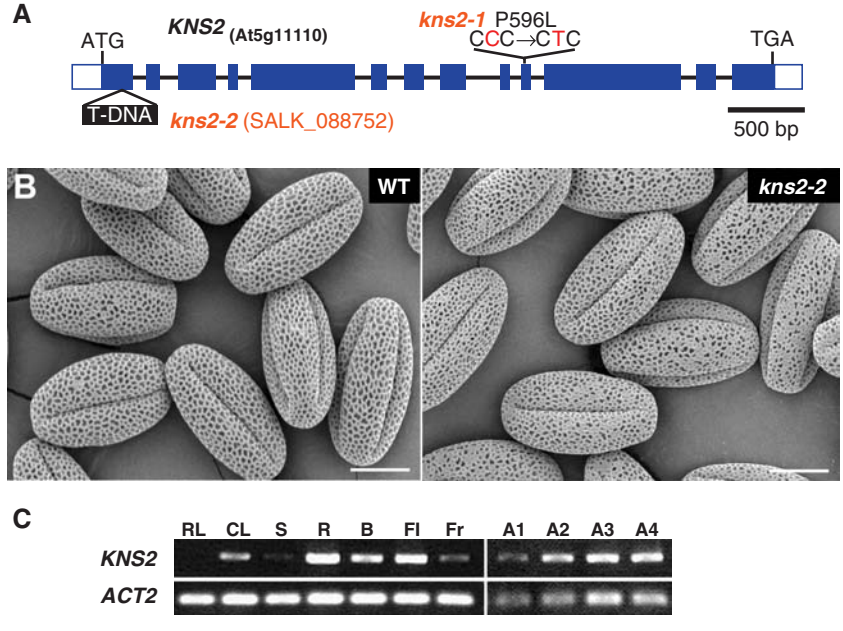

Fig. 6 Identification of the *KNS2* gene. (A) Schematic representation of *KNS2* gene structure. Exons are boxed. Filled boxes (blue) and open boxes (white) represent coding regions and untranslated regions, respectively. Thick lines (black) represent introns. Base substitutions in *kns2-1* and the T-DNA insertion in *kns2-2* are indicated. (B) Scanning electron micrographs of wild-type (Col-0) and *kns2-2* pollen grains. The mesh size of the reticulate structure in *kns2-2* exine is smaller than that of the wild type. Bars = 10 µm. (C) RT–PCR of the *KNS2* transcript. *ACT2* was used as a control. RL, rosette leaves; CL, cauline leaves; S, stems; R, roots; B, flower buds; Fl, opened flowers; Fr, fruits; A1, stage 10/11 anthers containing unicellular and bicellular microspores; A2, early stage 12 anthers containing bicellular microspores; A3, late stage 12 anthers containing tricellular pollen grains; A4, dehisced anthers of opened flowers carrying mature pollen grains.

artifact because such a structure could not be observed in samples that were prepared by a rapid freezing–freeze substitution method (Paxson-Sowders et al. 2001). Nevertheless, it seems likely that the pattern of probacula distribution is determined in this stage.

We isolated 12 mutants, *kns1–kns12*, showing abnormal exine structures in screening approximately 2,000 mutagenized M_2 plants. All these mutations are recessive and affect pollen development sporophytically, indicating that the genes are expressed in diploid cells, such as pollen mother cells and tapetal cells. However, most developmental events for exine formation occur at the surface of individual microspores, after meiosis of pollen mother cells has been completed. To explain this apparent discrepancy, many *KNS* genes are likely to be expressed in pollen mother cells, which transmit the mRNA or proteins to the microspores. Another possibility is that they are expressed in tapetal cells to produce exine components. Similar sporophytic effects have been observed in exine mutants *atmyb103/ms188*, *cyp703a2*, *dex1*, *flp1/wax2/yre/cer3*, *ms1/hkm*, *ms2*, *nef1*, *rpg1* and *tde1/det2*, all of which show defective exine formation and male sterility (Arrts et al. 1997, Paxson-Sowders et al. 2001, Ariizumi et al. 2003, Ariizumi et al. 2004, Ito et al. 2007, Morant et al. 2007, Yang et al. 2007, Zhang et al. 2007, Ariizumi et al. 2008, Guan et al. 2008). As expected, at least *CYP703A2*, *MS1/HKM*, *MS2*, *RPG1* and *TDE1/DET2* are expressed in tapetal cells or in both tapetal cells and pollen mother cells (Aarts et al. 1997, Morant et al. 2007, Yang et al. 2007, Ariizumi et al. 2008, Guam et al. 2008). In contrast, the *CalS5/LAP1* gene works gametophytically in microspores after meiosis (Dong et al. 2005).

Based on the characteristics of exine phenotype, *kns* mutations were classified into four types. Considering the proposed model for pollen wall development (Scott 1994, Owen and Makaroff 1995, Paxson-Sowders et al. 1997, Paxson-Sowders et al. 2001), we speculate on the function of *KNS* genes as follows (**Fig. 7**). The pollen grains of type 1 mutants, *kns1* and *kns11*, show highly collapsed exine structure and a distorted shape, which resembles the pollen phenotype of *cals5/lap1*, a mutation of the gene encoding callose synthase (Dong et al. 2005, Nishikawa et al. 2005). Together with the recessive nature of the *kns1* and *kns11* mutations, it is likely that *KNS1* and *KNS11* genes are expressed in pollen mother cells and are involved in biosynthesis or secretion of callose. The apparent male sterility of *kns11* also resembles that of *cals5/lap1*, although *kns1* shows normal fertility.

The type 2 mutants, for which we only have *kns4* at the moment, show a thin exine layer mainly due to shortened baculae. No such mutants have been reported previously. Although it is not known how the baculae elongates without disturbing the entire sexine structure during pollen development, it seems that their elongation is closely related to the thickening of primexine. Therefore, it is likely that *KNS4* is a novel gene regulating the thickening of the primexine layer (**Fig. 7**). Unlike the previously described mutation *nef1*, which affects primexine formation (Ariizumi et al. 2004), the *kns4* mutation has never been observed to disturb either pollen interior structure or pollen fertility.

Because the type 3 mutants, *kns5*, *kns6*, *kns7*, *kns8*, *kns9* and *kns10*, formed an incomplete tectum on the pollen surface, we assumed that these *KNS* genes are required for

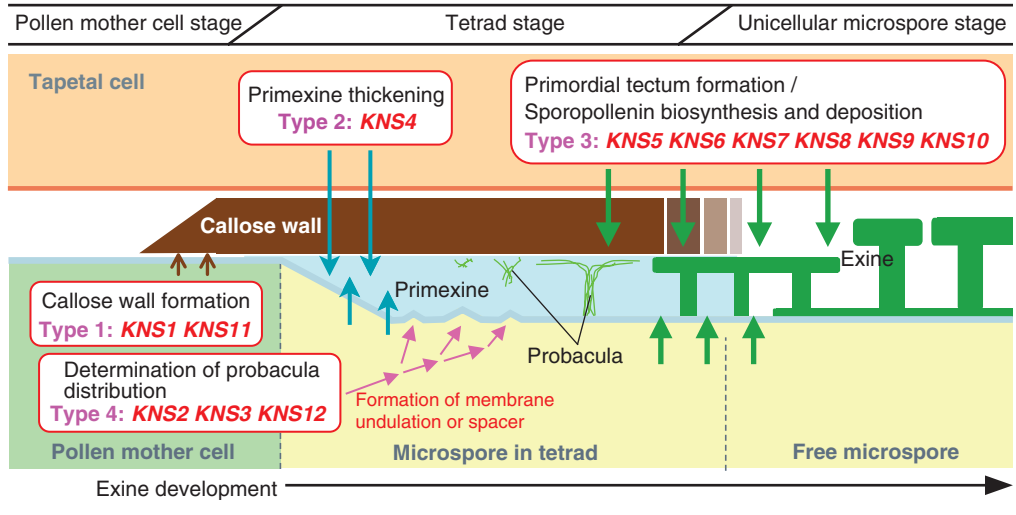

Fig. 7 Presumed functions of *KNS* genes. Schematic diagram of exine formation, which is based on previous models (Scott 1994, Paxon-Sowders et al. 1997), and predicted functions of the 12 *KNS* genes identified in this screening. The diagram indicates where expression of the genes is expected. Note that tapetal cells and pollen mother cells are diploid cells whereas microspores are haploid cells.

tectum formation. The tectum initially develops in the boundary between primexine and the callose wall, and connects the distal ends of probaculae. Deposition of sporopollenin onto the tectum continues even after dissolution of the callose wall, and the tectum grows into thick porous roofs of a reticulate exine structure. Therefore, we predict the following two possibilities for the function of type 3 genes (**Fig 7**): (i) they are required for creating primordial tectum, on which sporopollenin is deposited, at the space between primexine and the callose wall; or (ii) they are required for biosynthesis and deposition of sporopollenin onto growing tectum and/or growing baculae, which are necessary for adequate tectum formation. In the latter case, the genes might be expressed in tapetal cells and involved in biosynthesis, secretion and polymerization of sporopollenin. In many plant species, including wheat and rice, the tapetal cells produce Ubisch bodies (or orbicules) to transport tapetum-derived sporopollenin to developing exine (Huysmans et al. 1998). However, no such structure has been identified in Arabidopsis or other members of the Cruciferae. It would be interesting to investigate how Arabidopsis transports tapetum-derived sporopollenin without an Ubisch body.

The type 4 mutants show abnormal distribution of bacula location. All three mutants we identified, *kns2*, *kns3* and *kns12*, have pollen grains with formation of dense baculae. We found that the number of baculae is determined when the probaculae are formed above the protrusions of the undulating microspore plasma membrane at the tetrad stage. Although we have never observed any objects in the crypts of this membrane [referred to as 'spacers' in *B. campestris* and thought to determine the distribution of future interbacular cavities of exine (Fitzgerald et al. 1995)], the type 4 *KNS* genes might be responsible for formation of such spacers or establishment of the proper frequency of the plasma membrane undulation, which in turn ensures the proper distribution of the probaculae (**Fig. 7**).

Although many mutants have been reported in which exine has collapsed (*atmyb103*, *cyp703a2*, *dex1*, *ms2*, *nef1* and *rpg1*) (Aarts et al. 1997, Paxon-Sowders et al. 1997, Paxson-Sowders et al. 2001, Ariizumi et al. 2004, Morant et al. 2007, Zhang et al. 2007, Guan et al. 2008), we did not identify such mutants, probably due to a difference in screening strategy. We observed the surface structure of pollen grains isolated from each M_2 plant individually, whereas most of the reported mutants were initially isolated as male-sterile mutants. Considering that it would be unlikely to miss such male-sterile mutants in our screening, this discrepancy most probably reflects the existence of many potential mutations affecting exine structure, most of which do not cause male sterility. We identified 12 *kns* mutants among 2000 M_2 plants, suggesting that genes affecting exine phenotype are fairly common. Although our individual screening using SEM required a lot of time and effort, it was a highly successful method for identifying a variety of mutants with defective exine formation. Furthermore, none of the *kns* mutants showed any visible phenotype other than exine abnormality (even though *kns11* pollen was sterile), suggesting that these genes specifically function in exine formation.

It has been reported that lipophilic molecules constituting exine mediate pollen–stigma adhesion in Arabidopsis (Zinkl et al. 1999). However, we found that most *kns* mutants show normal or almost normal fertility, suggesting that such lipophilic molecules, if present, are in the pollen grains of all the *kns* mutants. Furthermore, it appeared that the correct reticulate structure of exine is not required for the interaction between pollen grains and stigmatic papillae.

We found that *KNS2* is identical to *AtSPS2F* and *AtSPS5.2* (At5g11110), which encodes SPS (Langenkamper et al. 2002, Lutfiyya et al. 2007), catalyzing the rate-limiting step of sucrose synthesis. Although there are four genes encoding SPS in the Arabidopsis genome, no mutations have previously been reported. The *kns2* mutant does not show any visible phenotype other than exine abnormality, although it is expressed in many organs. It is possible that the four *SPS* genes function redundantly during plant growth, with the exception of their roles in exine formation.

Pollen grains of the *kns2* mutant show a fine mesh pattern in the reticulate exine structure, and their tectum is occasionally broken into short fragments. Because the distribution of the baculae is determined at the tetrad stage, it is expected that *KNS2* would be expressed in young anthers around the tetrad stage. However, we have not confirmed its expression at this stage, because it is difficult to collect such young anthers. We detected *KNS2* expression in stage 10/11 anthers, which included unicellular and bicellular microspores, and the expression level increased at a later stage, suggesting that *KNS2* is involved in exine formation throughout the development of microspores. Alternatively, *KNS2* might be expressed in mature pollen grains and have a role in pollen fertility, although *kns2* pollen grains are fully fertile.

How SPS protein is involved in exine formation is largely unknown, although a correlation between SPS activity and the rate of cellulose synthesis has been reported (Babb and Haigler 2001). Sucrose availability in cellulose-synthetic cells affects the rate of cellulose biosynthesis, because the glucose units used for cellulose synthesis are UDP-glucose, which is supplied by degradation of sucrose. Therefore, increased availability of sucrose by accelerated SPS activity might enhance cellulose synthase activity. This idea is supported by experiments showing that overexpression of SPS improves fiber quality in cotton and Arabidopsis (Haigler et al. 2007, Park et al. 2008). Because of the structural similarity between callose synthase and cellulose synthase, SPS activity might also be important for callose synthesis. Therefore, KNS2 might be responsible for cellulose or callose

synthesis during microspore development, such as callose wall synthesis and primexine formation, both of which are required for probacula formation and sporopollenin deposition.

In this report, we described successful screening to identify mutations affecting exine formation. Gene identification and precise characterization of the mutations identified will help to uncover the molecular mechanism involved in the formation of the complex exine structure.

Materials and Methods

Plant materials and growth conditions

Arabidopsis thaliana (L.) Heinh. accession Ler was used as the wild type for observations by SEM and TEM. Accession Col-0 was used with all *kns* mutants for mapping crosses, and as the wild-type control in comparisons with *kns2-2*. *kns2-2* (SALK_088752, Col-0 background) was obtained from the Arabidopsis Biological Resource Center.

Seedlings were grown on agar plates of Gamborg B5 medium (Nihon Pharmaceutical, Tokyo, Japan) (Gamborg et al. 1968) supplemented with 1% sucrose for 2 weeks under continuous illumination at 22°C. The plants were then transplanted to vermiculite and grown under the above conditions.

Mutant screening

We used an EMS-mutagenized M_2 population of the Ler background (Lehle Seeds, Round Rock, TX, USA) for mutant screening. We detached one stamen from a fully opened flower of each M_2 plant and attached its pollen grains onto an adhesive carbon tab that covered the top surface of an aluminum SEM sample holder. These specimens were coated with Pt and Pd in an ion sputter (E-1030, Hitachi, Tokyo, Japan), and then observed by SEM (S-3000N microscope, Hitachi) at an accelerating voltage of 5 kV in high vacuum mode.

TEM observation

Flower buds were fixed in 3% glutaraldehyde in 50 mM Na-phosphate buffer (pH 7.2) overnight at 4°C, then in 0.14 M sucrose in 100 mM Na-phosphate buffer overnight at 4°C, and then in 1% osmium tetroxide solution in 0.21 M sucrose/50 mM Na-phosphate buffer for 2 h at 4°C. The sample was dehydrated in a graded ethanol series, treated with propylene oxide, and embedded in Spurr resin. Ultrathin sections 85 nm thick were prepared by an ULTRACUT N ultramicrotome (Reichert-Nissei, Tokyo, Japan) with a diamond knife and mounted on copper grids. The sections were then stained in 4% uranyl acetate for 20 min and lead citrate for 3–5 min. These specimens were viewed by TEM (H-7500AMT microscope, Hitachi).

Rough mapping of *kns* mutations

We crossed each *kns* mutant with the Col-0 wild type and selected F_2 plants by screening for abnormal exine structure by SEM. Genomic DNA from individual F_2 plants (~40 plants for rough mapping) was isolated and analyzed by simple sequence length polymorphism (SSLP) markers (Bell and Ecker 1994).

Map-based cloning of *KNS2*

Rough mapping of the *KNS2* locus was carried out as indicated above using SSLP markers listed in a public database (TAIR Marker Search, http://www.arabidopsis.org), and was mapped between two markers, CIW14 and CA72. For fine mapping, 1,114 F_2 plants were used for PCR analysis of CIW14 and CA72, and 58 plants were identified that had a recombination site between these two markers. Then, pollen phenotypes of these 58 plants were observed by SEM, and 24 plants homozygous and 21 plants heterozygous for the *kns2-1* mutation were identified. These 45 plants were used for further mapping using single nucleotide polymorphism (SNP) markers recorded in a database (TAIR Polymorphism/Allele Search, http://www.arabidopsis.org). For PCR analysis, the SNP markers were converted to derived cleaved amplified polymorphic sequence (dCAPS) markers (Neff et al. 1998). Finally, we determined the nucleotide sequence between PERL0881551 and PERL0882000 using an ABI 3130xl genetic analyzer and Big Dye Terminator Cycle Sequencing Kit ver. 3.1 (Applied Biosystems, Foster City, CA, USA) to identify the mutation corresponding to *kns2-1*.

To determine the 5′ and 3′ T-DNA insertion sites in *kns2-2*, DNA fragments including the junctions were amplified by PCR using the following primers: for the 5′ T-DNA insertion site, 5′-TTTTGTAGAGAGATTGGTTTCTGCT-3′ and 5′-TTTCGCCTGCTGGGGCAAACCAG-3′ (left border); and for the 3′ T-DNA insertion site, 5′-TCGTTGCGGTT CTGTCAGTTCC-3′ (right border) and 5′-TCTCAAAGACAT CAACAGAACTAAT-3′. Resulting PCR fragments were sequenced.

RT–PCR

Organs were harvested from soil-grown Col-0 plants and used for RNA preparation. To harvest anthers at each developmental stage, flower buds were classified into four stages (stage 10/11, early 12, middle 12 and late 12) according to the definition of Smyth et al. (1990). Stages early 12, middle 12 and late 12 represent green, yellowish green and yellow anthers, respectively. RNA was extracted from various organs using an RNeasy Plant Mini Kit (Qiagen, Hilden, Germany), and used for cDNA synthesis using SuperScript III reverse transcriptase (Invitrogen, Carlsbad, CA, USA) and oligo$(dT)_{20}$ primer. PCR was carried out using Ex Taq polymerase (TAKARA BIO INC., Otsu, Japan). Primers used for PCR were

as follows: *KNS2*, 5′-ATTCTCTCAACCTCAATGACAATAT-3′ and 5′-AAGTCACTGGCTAAGCCTTTAA-3′; *ACT2*, 5′-CTGT TGACTACGAGCAGGAGATGGA-3′ and 5′-GACTTCTGGG CATCTGAATCTCTCA-3′.

Funding

The Ministry of Education, Culture, Sports, Science, and Technology (MEXT), Japan (17051013 and 19043008 to S.I.); Japan Society for the Promotion of Science (JSPS) (20000304 to T.S.); Global COE Program 'Advanced Systems-Biology: Designing the Biological Function', MEXT, Japan. T.S. received support from the Research Fellowship for Young Scientists from JSPS.

Acknowledgments

We thank Dr. Hiroshi Miyake (Nagoya University) and Drs. Mikio Nishimura and Maki Kondo (National Institute for Basic Biology) for instruction on observation by TEM, and Ms. Terumi Nishii for excellent technical assistance.

References

Aarts, M.G., Hodge, R., Kalantidis, K., Florack, D., Wilson, Z.A., Mulligan, B.J., et al. (1997) The Arabidopsis *MALE STERILITY 2* protein shares similarity with reductases in elongation/condensation complexes. *Plant J.* 12: 615–623.

Ariizumi, T., Hatakeyama, K., Hinata, K., Inatsugi, R., Nishida, I., Sato, S., et al. (2004) Disruption of the novel plant protein NEF1 affects lipid accumulation in the plastids of the tapetum and exine formation of pollen, resulting in male sterility in Arabidopsis thaliana. *Plant J.* 39: 170–181.

Ariizumi, T., Hatakeyama, K., Hinata, K., Sato, S., Kato, T., Tabata, S., et al. (2003) A novel male-sterile mutant of *Arabidopsis thaliana*, *faceless pollen-1*, produces pollen with a smooth surface and an acetolysis-sensitive exine. *Plant Mol. Biol.* 53: 107–116.

Ariizumi, T., Hatakeyama, K., Hinata, K., Sato, S., Kato, T., Tabata, S., et al. (2005) The *HKM* gene, which is identical to the *MS1* gene of Arabidopsis thaliana, is essensial for primexine formation and exine pattern formation. *Sex. Plant Reprod.* 18: 1–7.

Ariizumi, T., Kawanabe, T., Hatakeyama, K., Sato, S., Kato, T., Tabata, S., et al. (2008) Ultrastructural characterization of exine development of the *transient defective exine 1* mutant suggests the existence of a factor involved in constructing reticulate exine architecture from sporopollenin aggregates. *Plant Cell Physiol.* 49: 58–67.

Babb, V.M. and Haigler, C.H. (2001) Sucrose phosphate synthase activity rises in correlation with high-rate cellulose synthesis in three heterotrophic systems. *Plant Physiol.* 127: 1234–1242.

Bell, C.J. and Ecker, J.R. (1994) Assignment of 30 microsatellite loci to the linkage map of Arabidopsis. *Genomics* 19: 137–144.

Dong, X., Hong, Z., Sivaramakrishnan, M., Mahfouz, M. and Verma, D.P. (2005) Callose synthase (CalS5) is required for exine formation during microgametogenesis and for pollen viability in Arabidopsis. *Plant J.* 42: 315–328.

Fitzgerald, M.A. and Knox, R.B. (1995) Initiation of primexine in freeze-substituted microspores of *Brassica campestris*. *Sex. Plant Reprod.* 8: 99–104.

Gamborg , O.L., Miller, R.A. and Ojima, K. (1968) Nutrient requirements of suspension cultures of soybean root cells. *Exp. Cell Res.* 50: 151–158.

Guan, Y.F., Huang, X.Y., Zhu, J., Gao, J.F., Zhang, H.X. and Yang, Z.N. (2008) *RUPTURED POLLEN GRAIN1*, a member of the MtN3/ saliva gene family, is crucial for exine pattern formation and cell integrity of microspores in Arabidopsis. *Plant Physiol.* 147: 852–863.

Haigler, C.H., Singh, B., Zhang, D., Hwang, S., Wu, C., et al. (2007) Transgenic cotton over-producing spinach sucrose phosphate synthase showed enhanced leaf sucrose synthesis and improved fiber quality under controlled environmental conditions. *Plant Mol. Biol.* 63: 815–832.

Huysmans, S., El-Ghazaly, G. and Smets, E. (1998) Orbicules in angiosperms: morphology, function, distribution, and relation with tapetum types. *Bot. Rev.* 64: 240–272.

Ito, T., Nagata, N., Yoshiba, Y., Ohme-Takagi, M., Ma, H. and Shinozaki, K. (2007) *Arabidopsis MALE STERILITY1* encodes a PHD-type transcription factor and regulates pollen and tapetum development. *Plant Cell* 19: 3549–3562.

Langenkämper, G., Fung, R.W., Newcomb, R.D., Atkinson, R.G., Gardner, R.C. and MacRae, E.A. (2002) Sucrose phosphate synthase genes in plants belong to three different families. *J. Mol. Evol.* 54: 322–332.

Lutfiyya, L.L., Xu, N., D'Ordine, R.L., Morrell, J.A., Miller, P.W. and Duff, S.M. (2007) Phylogenetic and expression analysis of sucrose phosphate synthase isozymes in plants. *J. Plant Physiol.* 164: 923–933.

McCormick, S. (1993) Male gametophyte development. *Plant Cell* 5: 1265-1275.

Morant, M., Jørgensen, K., Schaller, H., Pinot, F., Müller, B.L., Werck-Reichhart, D., et al. (2007) CYP703 is an ancient cytochrome P450 in land plants catalyzing in-chain hydroxylation of lauric acid to provide building blocks for sporopollenin synthesis in pollen. *Plant Cell* 19: 1473–1487.

Neff, M.M., Neff, J.D., Chory, J. and Pepper, A.E. (1998) dCAPS, a simple technique for the genetic analysis of single nucleotide polymorphisms: experimental applications in Arabidopsis thaliana genetics. *Plant J.* 14: 387–392.

Nishikawa, S., Zinkl, G.M., Swanson, R.J., Maruyama, D. and Preuss, D. (2005) Callose (beta-1,3 glucan) is essential for Arabidopsis pollen wall patterning, but not tube growth. *BMC Plant Biol.* 5: 22.

Owen, H.A. and Makaroff, C.A. (1995) Ultrastructure of microsporogenesis and microgametogenesis in *Arabidopsis thaliana* (L.) Heynh. ecotype Wassilewskija (Brassicaceae). *Protoplasma* 185: 7–21.

Park, J.Y., Canam, T., Kang, K.Y., Ellis, D.D. and Mansfield, S.D. (2008) Over-expression of an arabidopsis family A sucrose phosphate synthase (SPS) gene alters plant growth and fibre development. *Transgenic Res.* 17: 181–92.

Paxson-Sowders, D.M., Dodrill, C.H., Owen, H.A. and Makaroff, C.A. (2001) DEX1, a novel plant protein, is required for exine pattern formation during pollen development in Arabidopsis. *Plant Physiol.* 127: 1739–1749.

Paxson-Sowders, D.M., Owen, H.A. and Makaroff, C.A. (1997) A comparative ultrastructural analysis of exine pattern development

in wild-type Arabidopsis and a mutant defective in pattern formation. *Protoplasma* 198: 53–65.

Rowland, O., Lee, R., Franke, R., Schreiber, L. and Kunst, L. (2007) The *CER3* wax biosynthetic gene from *Arabidopsis thaliana* is allelic to *WAX2/YRE/FLP1*. *FEBS Lett.* 581: 3538–3544.

Scott, R.J. (1994) Pollen exine: the sporopollenin enigma and the physics of pattern. *In* Molecular and Cellular Aspects of Plant Reproduction. Edited by Scott, R.J. and Stead, M.A. pp. 49–81. Cambridge University Press, Cambridge.

Scott, R.J., Spielman, M. and Dickinson, H.G. (2004) Stamen structure and function. *Plant Cell* 16: S46–S60.

Smyth, D.R., Bowman, J.L. and Meyerowitz, E.M. (1990) Early flower development in Arabidopsis. *Plant Cell* 2: 755–767.

Yang, C., Vizcay-Barrena, G., Conner, K. and Wilson, Z.A. (2007) MALE STERILITY1 is required for tapetal development and pollen wall biosynthesis. *Plant Cell* 19: 3530–3548.

Zhang, Z.B., Zhu, J., Gao, J.F., Wang, C., Li, H., et al (2007) Transcription factor *AtMYB103* is required for anther development by regulating tapetum development, callose dissolution and exine formation in Arabidopsis. *Plant J.* 52: 528–538.

Zinkl, G.M., Zwiebel, B.I., Grier, D.G. and Preuss, D. (1999) Pollen–stigma adhesion in *Arabidopsis*: a species-specific interaction mediated by lipophilic molecules in the pollen exine. *Development* 126: 5431–5440.

(Received August 2, 2008; Accepted August 29, 2008)